RSC Advances

ROYAL SOCIETY OF CHEMISTRY

www.rsc.org/advances

RSC Advance

ARTICLE

Novel redox-responsive nanogel based on poly(ionic liquid)s for the triggered loading and release of cargos

Received 00th January 20xx,
Accepted 00th January 20xx

DOI: 10.1039/x0xx00000x

www.rsc.org/

Congcong Miao,[a] Feng Li,[a] Yong Zuo,[a] Rongmin Wang,[a] and Yubing Xiong[a,b]

The unique disulfide chemistry has been widely explored for novel and versatile delivery systems addressing both intracellular and extracellular barriers. In this study, novel redox-responsive nanogels were fabricated by radical copolymerization of ionic liquid (IL)-based monomers, 1,n-butanediyl-3,3'-bis-1-vinylimidazolium dibromide ([C_nVIm]Br, n=4,6), and disulphide dimethacrylate (DSDMA) in selective solvent. The as-synthesized nanogels were characterized using scanning electron microscopy (SEM), Fourier transform infrared (FTIR), thermogravimetric analyses (TG), dynamic laser scattering (DLS) and zeta (ζ)-potential measurements. The results demonstrated that the sizes of poly(ionic liquid) (PIL)-based nanogels can be tuned by the feed ratio of the monomers and DSDMA. Moreover, the redox-response performances of these nanogels were evaluated through the size varieties in the presence of dithiothreitol (DTT) and benzoyl peroxide (BPO). The capability of PIL-based nanogels for controlled release was also investigated by using Rhodamine B (RhB) as prototype model drug. It was found that DTT-triggered release of RhB could be achieved. Therefore, a redox-triggered loading and release matrix can be conveniently fabricated via PIL-based nanogels. And it can also be potentially used as controlled carrier in biological medicine.

Introduction

Smart nanomaterials, which can respond quickly to the environmental stimuli, such as temperature, light, electricity, ultrasound, magnetic fields, enzymes, pH, electrolytes and redox potential etc., have generated tremendous interests in the past several decades due to their potential fundamental and industrial applications.[1-7] In these various stimuli-responses, redox-response has drawn increasing attention because they contain redox-responsive polymers with a high redox potential difference (100-1000 fold) between the reducing intracellular space and the oxidizing extracellular space.[8-12] These interesting features enable them to be promising candidates for controlled drug delivery system with optimized drug loading and releasing, prolonged circulation time, and accurate targeting.[13-17]

Moreover, it is well-known that the significant difference of redox potential between the extracelluar and intracellular compartments is due to the existence of high concentration glutathione (GSH).[18] Till now, many studies have been focusing on the utilization of disulfide-functionalized linkages to build redox-responsive matrixes for controlling the biodegradability and drug release[19-25]. Recently, polymeric nanomaterials, especially nanogels, have been widely developed as the matrix with all kinds of stimuli-response.[26,27] Although the recent reports have demonstrated a great potential of redox-responsive nanogels as drug and catalyst carriers or nanoreactors, multiple functional nanogels for practical applications remain an active research field because of the difficulties in facile clean preparation, uniformity in shape and network, and well surface modification that arises from the complicated polymerization and post-treatment procedures.[28,29]

Ionic liquids (ILs), composed entirely of ions in the liquid state below 100 °C, have garnered extensive attention in a variety of fields. The current interests in ILs are motivated by their unique properties, including negligible vapor pressure, thermal stability, high polarity, solvating characteristics, non-flammability, high ionic conductivity, and a wide electrochemical stability window.[30-35] Recently, it has been found to be a significant topic on the design of poly(ionic liquid) (PIL) bearing thermoresponsive phase behavior in water and other solvents.[36-38] In the previous studies, our group has demonstrated a facile one-step synthesis strategy to prepare PIL-based nanogels via the conventional radical copolymerization of IL-based monomers and the cross-linkers ethylene glycol dimethacrylate (EGDMA) and divinylbenzene (DVB) in selective solvents.[39,40] In addition, thermo-responsive nanogels could also be prepared for the first time via the copolymerization of the geminal dicationic, 1,n-butanediyl-3,3'-bis-1-vinyl imidazolium halides (n = 4, 6, 8, 12), and the cross-linkers described above under the same conditions.[41,42]

[a] Key Laboratory of Eco-Environment-Related Polymer Materials, Ministry of Education; College of Chemistry and Chemical Engineering, Northwest Normal University, Lanzhou 730070, China.
[b] Max Planck Institute for Polymer Research, Ackermannweg 10, Mainz 55128, Germany.

† Footnotes relating to the title and/or authors should appear here.

Electronic Supplementary Information (ESI) available: [details of any supplementary information available should be included here]. See DOI: 10.1039/x0xx00000x

To endow PIL-based nanogels with more performances, herein, disulfide-functionalized cross-linker, disulphide dimethacrylate (DSDMA), was synthesized and copolymerized with biimidazolium ionic liquid (BImIL)-based monomers, [C_nVIm]Br (n=4, 6), in selective solvent. Therefore, novel redox-responsive nanogels can be obtained, and the sizes of these PIL-based nanogels can be tuned by reductant and oxidant. Additionally, model drug Rhodamine B (RhB) can be loaded and released controllably by the redox-responsive nanogels.

Experimental

Materials and methods

All the reagents were purchased from commercial supplier. Vinyl imidazole (VIm, 99%) was distilled on vacuum to remove the inhibitor before use. Azobisisobutyronitrile (AIBN) was recrystallized from methanol before use. All other chemicals were used without further treatment.

Fourier transform infrared (FT-IR) spectra were recorded on a DIGIL FTS3000 spectrophotometer using KBr tablets. ^{1}H and^{13}C NMR spectra were recorded on a Brucker AM 400 MHz spectrometer at 25 °C. Thermogravimetric analyses (TGA) were measured on a Perkin Elmer TG/TGA 6300 at a heating rate of 10 °C min^{-1}. Differential scanning calorimetry (DSC) measurements were recorded on a DSC 822e thermal analysis system (Mettler Toledo Instruments Inc. Switzerland) at a heating rate of ±1 °C/min with nitrogen protected (80 ml min^{-1}). The morphology of nanogels was observed by scanning electron microscopy (SEM, JSM 6700F, Japan). Dynamic laser scattering (DLS) measurements were carried out on a commercial laser light scattering instrument (Malvern Autosizer 4700, Malvern Instruments) at 25 °C and 90° scattering angle. The measured time correlation function was analyzed by the automatic program equipped with the correlator. The z-average hydrodynamic diameter (D_h) and polydispersity index (PDI, μ_2/Γ^2) were obtained by CONTIN mode analysis.[43,44] Zeta (ζ)-potential measurements were performed on a ZetaSizer Nano ZS90 (Malvern Instruments). Electrophoresis mobility was measured and ζ-potential was calculated by the Dispersion Technology Software provided by Malvern according to Henry equation: $U_E = (2\varepsilon\zeta/3\mu)f(\mathrm{ka})$, where ε, μ, f(ka) are the dielectric permittivity of the solvent, viscosity of the solution, and Henry's function, respectively.[45] The elemental analyses (EA) are measured directly without any additives using a Vario EL Cube (Elementar Analysensysteme, Germany), and Mass Spectroscopy (MS) were performed using water as the solvent without additives on a micrOTOF-QII mass spectrometer (Bruker Company, USA).

Synthesis of 1,4-butanediyl-3,3'-bis-1-vinylimidazolium dibromide ([C_4VIm]Br).

1,4-Butanediyl-3,3'-bis-1-vinylimidazolium dibromide ([C_4VIm]Br) was synthesized according to literature.[41,42] Vinyl imidazole (Vim, 4.00 g, 42.5 mmol) and 1,4-dibromobutane (4.75 g, 20 mmol) were dissolved in methanol (50 mL) in a round-bottom flask fitted with a condenser and N_2 bubbler. Subsequently, the mixture was stirred at 70 °C for 48 hrs under nitrogen atmosphere. After then, the reaction solution was precipitated from diethyl ether (150 mL), and the solid was dissolved in methanol and precipitated from diethyl ether two times. The obtained product was dried under vacuum for 24 h at R.T. [C_4VIm]Br was obtained as white solid (Yield: 5.3 g, 65.6%). mp: 150–151 °C. ^{1}H NMR (D_2O, 400 MHz, ppm): 7.59(1H, d), 7.39(1H, d), 6.94(1H, m), 5.59(1H, m), 5.24(1H, m), 4.12(2H, s), 1.78(2H, s). ^{13}C NMR(D_2O, 100 MHz, ppm): 134.61, 128.49, 123.10, 119.91, 109.62, 49.34, 26.31. ESI-MS (m/z): Calcd. for $C_{14}H_{20}N_4Br_2$: 404.15; Found: 404.1. EA (%): Calcd. for: C, 41.61, H, 4.99, N, 13.86, Br, 39.54; Found: C, 40.53, H, 5.34, N, 13.55, Br, 40.58.

Synthesis of 1,6-hexanediyl-3,3'-bis-1-vinylimidazolium dibromide ([C_6VIm]Br).

1,6-Butanediyl-3,3'-bis-1-vinylimidazolium dibromide ([C_6VIm]Br) was prepared according to the similar method. [C_6VIm]Br was obtained as white solid (Yield: 6.2 g, 64.8%). mp: 219 °C. ^{1}H NMR(D_2O, 400 MHz, ppm): 7.57(1H, s), 7.37(1H, s), 6.93(1H, m), 5.60(1H, d), 5.22(1H, d), 4.04(2H, t), 1.70(2H, s), 1.17(2H, s). ^{1}H NMR(DMSO, 400 MHz, ppm): 9.66(1H, s), 8.24(1H, t), 7.99(1H, t), 7.33(1H, m), 5.99(1H, m), 5.43(1H, m), 4.22(2H, t), 1.83(2H, d), 1.31(2H, s). ^{13}C NMR(DMSO, 100 MHz, ppm): 135.36, 128.88, 123.31, 119.23, 109.04, 49.02, 28.80, 24.77. ESI-MS (m/z): Calcd. for $C_{16}H_{24}N_4Br_2$: 432.2; Found 432.2. EA (%): Calcd. C, 44.46; H, 5.60; N, 12.96; Br, 36.98. Found: C, 42.94; H, 5.36; N, 12.50; Br, 39.20.

Synthesis of Disulphide dimethacrylate (DSDMA).

Disulphide dimethacrylate (DSDMA), was synthesized according to the literature.[46] In a typical reaction, bis-(2-hydroxyethyl) disulphide (BHEDS, 10.00 g, 64.84 mmol) and triethylamine (54 mL, 38 mmol) were dissolved in anhydrous dichloromethane (150 mL) in a round-bottom flask equipped with a stirrer, a thermometer, and dripping funnel. Then, the flask was immersed in an ice bath (0–5 °C), and methacryloyl chloride (MAC, 20.08 g, 192.09 mmol) was added dropwise. The reaction continued for 30 min at 0 °C, and another 24 h at room temperature. After then, the reaction was stopped and triethylamine hydrochloride was removed by filtration. The solvent in the filtrate was eliminated through rotary evaporation. Yellow liquid was obtained and washed with sodium carbonate aqueous solution and water three times, respectively. The organic phase was dried with anhydrous magnesium sulfate, and the crude product was purified by silica gel column chromatography (eluant: dichloromethane : petroleum ether = 2:1, v:v). Finally, DSDMA was obtained as a lightly yellow transparent liquid (Yield: 76%) and was stored in a fridge in the absence of light prior to use. ^{1}H NMR($CDCl_3$, 400 MHz, ppm): 6.14(2H, s), 5.59(2H, d), 4.41(4H, t), 2.98(4H, t), 1.95(6H, s). ^{13}C NMR($CDCl_3$, 100 MHz, ppm): 166.90, 135.90, 125.79, 62.36, 37.21, 18.11. All the NMR spectra were provided in the supporting information (Figure S1-S7).

Preparation of redox-responsive polymeric nanogels.

Redox-responsive polymeric nanogels were synthesized via cross-linking copolymerization of imidazolium ionic liquid-based monomers [C_nVIm]Br (n=4, 6) and the cross-linkers DSDMA using AIBN as initiator in selective solvents.[41] The

following protocol is representative of all nanogel syntheses. [C_4VIm]Br (0.57 g, 1.40 mmol), DSDMA (0.043 g, 0.14 mmol), and AIBN (8.3 mg, 0.051 mmol) were dissolved in methanol (30 mL), and the solution was stirred at 70 °C for 12 h. After the polymerization was quenched by immersing into ice/water mixture, the reaction solution was precipitated from diethyl ether (150 mL), and the solid product was washed using THF, and diethyl ether, respectively. The products were dried under vacuum for 24 h at 50 °C. (Yield: 67%). [C_6VIm]Br-based nanogels were prepared according to the similar process.

Redox-triggered decross-linking and recross-linking of BImIL-based nanogels.

The hydrodynamic diameter (D_h) varieties of BImIL-based nanogels in response to reductant dithiothreitol (DTT) and oxidant benzoyl peroxide (BPO) was monitored by dynamic light scattering (DLS) measurement. Briefly, 5 mg nanogels were dispersed into 10 mL phosphate buffer (10 mM, pH 7.4) solution under sonication, and then 5 mg DTT was added. The solution was stirred at room temperature under nitrogen atmosphere. At predetermined intervals, samples were collected and their D_h were determined using DLS. After 24 hrs, the oxidant BPO (10 mg) was added, and the solution was stirred under air for another 24 hrs. Finally, samples were collected and their D_h were measured using DLS.

Drug encapsulation and redox-triggered drug release.

Rhodamine B (RhB) was selected as the model drug to investigate the redox-triggered drug loading and release behavior of BImIL-based nanogels. Typically, dried nanogel (0.50 g) was dispersed in 30 mL of phosphate buffer solution (pH 7.4) by low-power bath sonication (50 w) for 30 min at room temperature. Then, DTT (100 mg) and RhB (50 mg) were added, and the solution was stirred gently under nitrogen atmosphere for 24 h. After that, BPO (150 mg) was added and the solution was stirred for another 24 h. The free RhB in the solution was separated from the nanogels by a highflow ultrafiltration membrane (cutoff molecular weight 10 kDa; MicroconYM-10, Millipore) and was collected in the ultrafiltrate. The adsorption of RhB on the ultrafiltration membrane was calibrated by a standard free RhB solution at the same condition. The absorption at 552 nm of the ultrafiltrate was measured on a TU-1901 spectrophotometer (Purkinje General Instrument Co., Ltd, Beijing, China) to calculate the free RhB concentration. The working curve was obtained by standard RhB solutions with different concentrations. The loading efficiency and loading amount were calculated using the following equations:

$$\mathrm{DLC}(\%) = \frac{\text{initial weight of RhB} - \text{weight of RhB in supernatant}}{\text{weight of RhB loaded nanogel}} \times 100\%$$

$$\mathrm{DLE}\ (\%) = \frac{\text{weight of RhB in nanogel}}{\text{initial weight of RhB}} \times 100\%$$

Free RhB in the solution was separated by dialyzation, and RhB-loaded nanogels were obtained by lyophilization. The release of RhB is conducted in a phosphate buffered saline (PBS) solution (pH 7.4). In each sample, a membrane tubing (molecular weight cut off 14,000), containing RhB-loaded nanogels (0.10 g) dispersed in PBS solution (5 mL), dialyzed against 20 mL PBS solution at 37 °C in a 30 mL serum bottle with gently shaken (200 rpm). The drug release was assumed to start as soon as the dialysis bags were placed into the reservoir. At predetermined periods, 4 mL of the solution was obtained periodically from the reservoir, and 4 mL fresh phosphate buffer solution (pH 7.4) was added into the reservoir. Four hours later, 5 mmol DDT was added, and the samples were taken out as previous manipulations. The absorption at 552 nm of the release buffer was measured to calculate the RhB concentration as described above. All RhB release data were averaged over three measurements.

Results and discussion

As demonstrated in our previous studies,[39-42] one-step cross-linking copolymerization of IL-based monomers is an efficient tactics to prepare functional nanogels, as well as thermo-responsive nanogels by introducing hydrogen (H)-bonding interactions. To explore more possibility of stimuli-responsive nanogel via one-step synthesis, disulfide-functionalized cross-linker, disulphide dimethacrylate (DSDMA), was used to copolymerize with biimidazolium-based monomers. As illustrated in Scheme 1, both of the monomers contain two polymerizable vinyl double bonds. Normally, the as-prepared polymers either precipitate or gelate in the absence of stabilizer. However, when these two monomers were copolymerized in methanol, stable nanogel solution could be obtained (as the photo showed in Scheme 1). Therefore, it is believed that the polymerization process is regulated by a similar mechanism in the previous reports.[39,42] That is, poly(BImIL) segments in the copolymer can stabilize the nanogels due to their high affinity to the solvent, and the polymerization process follows the mechanism of disperse polymerization.

Dynamic laser scattering (DLS) was used to investigate the hydrodynamic diameter (D_h) of the as-prepared nanogels. The results are summarized in Table 1. As it shows, D_h of these nanogels are in the range of 25 nm to 310 nm with the various feed ratio of BImIL and DSDMA. And the diameter of nanogels increases with increasing BImIL in feed. Too less BImIL in the feed (less than 5:1) will result in the precipitation of particles from the solvent, because the particles cannot be stabilized by BImIL segments in the copolymers. When the feed ratio is higher than 15:1, the diameter of nanogels with [C_4VIm]Br monomer is significantly larger than [C_6VIm]Br monomer.

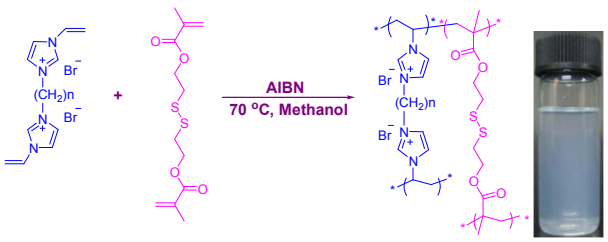

Scheme 1 Schematic illustration of one-step synthesis of BImIL-based nanogels (n=4, 6, the inset photo shows the as-prepared nanogel solution).

Table 1. Influence of various feed ratio on sizes of BVIm-based nanogels.[a]

Entry	Monomer	Feed ratio[b]	D_h (nm)	PDI	Zeta (mV)
NG1	[C_4VIm]Br	5:1	25	0.632	6.8
NG2	[C_4VIm]Br	10:1	65	0.592	7.3
NG3	[C_4VIm]Br	15:1	214	0.273	14.4
NG4	[C_4VIm]Br	20:1	304	0.645	14.2
NG5	[C_6VIm]Br	5:1	40	0.190	7.2
NG6	[C_6VIm]Br	10:1	93	0.120	8.5
NG7	[C_6VIm]Br	15:1	105	0.396	11.8
NG8	[C_6VIm]Br	20:1	217	0.422	11.9
NG9	[C_6VIm]Br	30:1	263	0.296	11.3

[a] polymerization conditions: ([Monomer] + [Cross-linker])/[AIBN]=30, in 30 mL methanol, 70 °C, 12 h; [b] molar ratio of [C_nVIm]Br to DSDMA; D_h: hydrodynamic diameter, PDI: polydispersity index of nanogels.

It is probably because [C_4VIm]Br is more affinitive to the solvent, As a result, it can stabilize the particles more efficiently which benefits to the growth of nanogels in the polymerization process. In addition, the higher PDI indicates that the BImIL-based nanogels are in wide dispersion, which is consistent with the previous studies. All the nanogels are very stable in the solution because they are positively charged.

The morphologies of BImIL-based nanogels were also examined using scanning electron microscope (SEM). As shown in Figure 1 and Figure S8 in the supporting information, the nanogels with spherical morphology are well-dispersed in the substrate. Moreover, their sizes are in the range of 20 to 200 nm, which are smaller than those measured by DLS. It is because DLS provides the results of swollen nanogels in the solution, whereas SEM gives the results of dried nanogels.

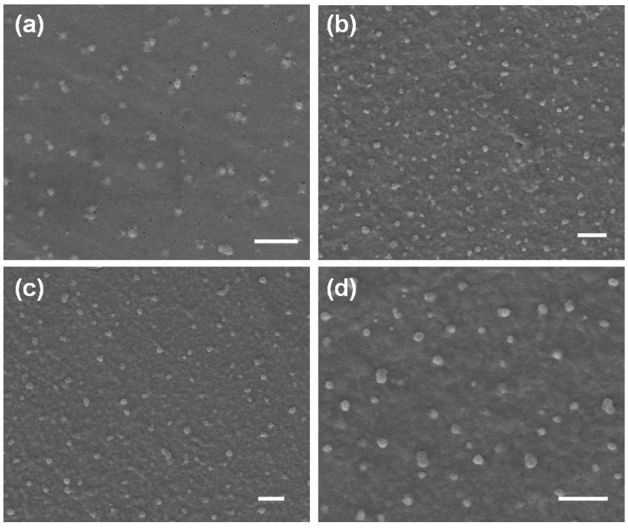

Figure 1 Typical SEM images of BImIL-based nanogels (a NG3; b NG5; c NG6; d NG9; All the scale bar are 1 μm).

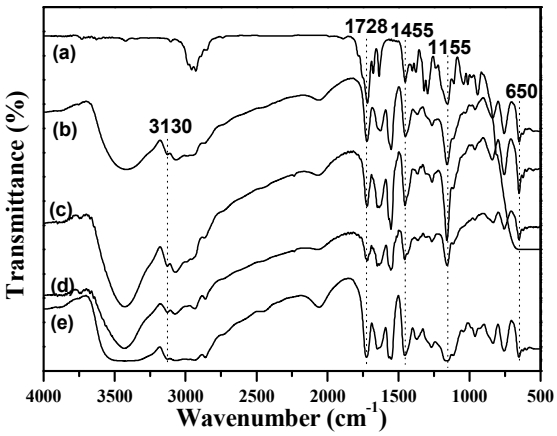

Figure 2 FTIR spectra of DSDMA and BImIL-based nanogels (a DSDMA; b NG4; c NG2; d NG9; e NG6).

Infrared spectra (FTIR) of BImIL-based nanogels are shown in Figure 2. Some typical peaks attributed to BIm-based IL and DSDMA copolymer can be clearly recognized, such as aromatic benzene ring (1646, 1500 cm^{-1}, stretching vibration), aromatic imidazolium ring (1454, 1180 cm^{-1} stretching vibration), carbonyl group (1728 cm^{-1}, stretching vibration), etc. Especially, a weak absorption at 650 cm^{-1} ascribed to the absorption peak of the disulfide bonds can also be observed. At the same time, the peak ascribed to the carbon-carbon double bond (1582 cm^{-1}, stretching vibration) in the vinyl group of the monomers disappeared. These results demonstrate the formation of BImIL and DSDMA copolymers. Furthermore, thermo-stabilities of the as-prepared nanogels were determined using thermogravimetric analysis (TGA). As illustrated in Figure 3, these BImIL-based copolymers are stable below 250 °C, which may be due to their highly cross-linked structure. However, the onset decomposition temperature (T_{dec}) of [C_4VIm]Br-based nanogels (about 280 °C) are lower than those of [C_6VIm]Br-based nanogels (about 290 °C). Disulfide bond contained compound are extensively utilized to fabricate redox-responsive matrixes. Therefore, the as-prepared nanogels are definitely redox-responsive. Under the reduce condition, the disulfide bonds can be cleaved and the nanogel will get bigger because of the less cross-linking points. On the contrary, the nanogel will become smaller due to formation of disulfide bonds in the presence of oxidant (as illustrated in Scheme 2). By utilizing the redox-triggered transformation in size of BImIL-based nanogels, Rhodamine B (RhB), due to its hydrophilicity and ionic structure, was selected as the model drug to investigate the loading and release performance in the

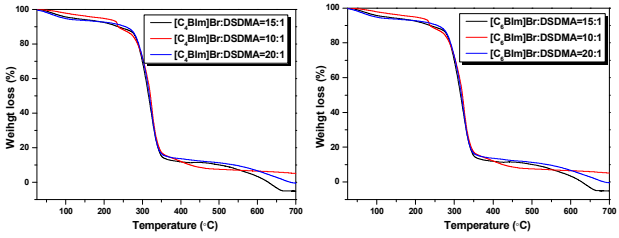

Figure 3 TGA curves of BImIL-based nanogels with different composition.

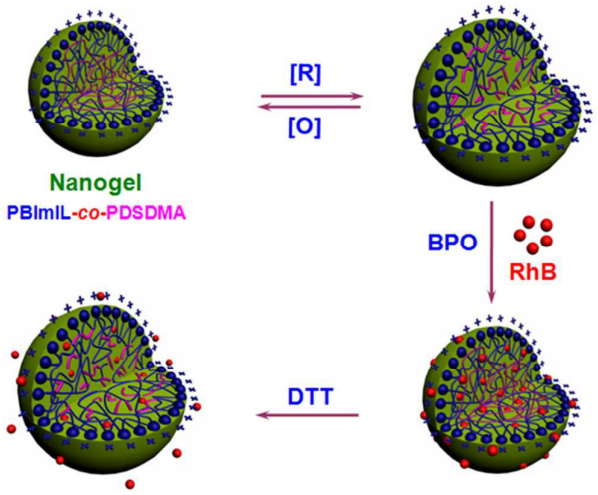

Scheme 2 Schematic illustration of redox-triggered drug loading and release of BImIL-based nanogel.

presence of reducing agent and oxidant, respectively. As a result, a novel redox-triggered drug loading and release matrix could be achieved conveniently through one-step synthesis of IL-based nanogels.

To testify the above possible redox-responsive performances of BImIL-based nanogels, the size variation of these nanogels in response to DTT and BPO in PBS (pH 7.4) solution was investigated using DLS measurement. As shown in Figure 4, the size of all these nanogels increases when incubated with 3.2 mM DTT in PBS solution for 2 h. With the incubation time extended, these nanogels become larger and

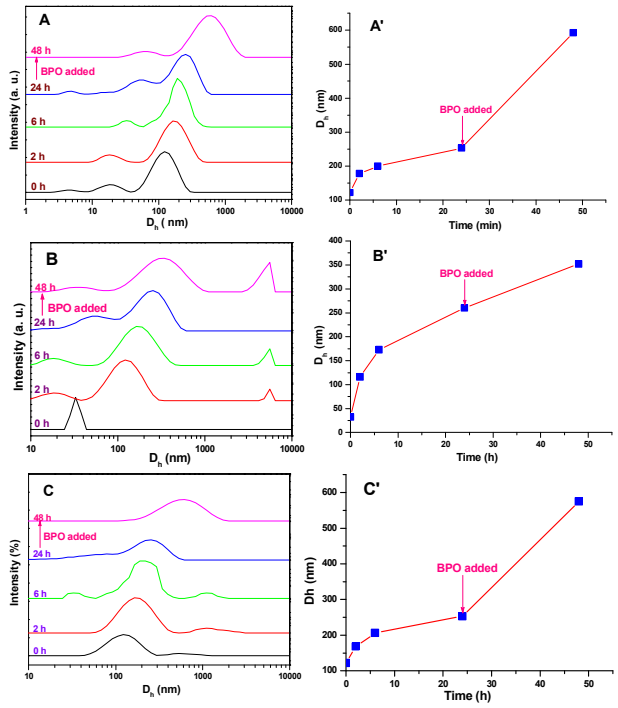

Figure 4 Size varieties of BImIL-based nanogels under redox conditions (pH=7.4 buffer solution). (A and A′ NG4; B and B′ NG7; C and C′ NG9)

larger. This variation in size is definitely because of the cleavage of disulfide bonds of PDSDMA in the reductive environment, which results in the swollen of BImIL-based nanogels by solvent. Especially, because of the high hydrophiphilicity of BImIL, the size of NG7 can become as large as 7 times of original particles. When these nanogels with cleaved disulfide bonds were incubated with BPO for another 24 h, it can be found that the sizes increased significantly, and particles in the submicrometer are obtained. However, BPO has been found to induce tumor and inflammatory responses in *vivo*.[47,48] A bio-friendly oxidant should be employed in the future applications. The performance of BVIm-based nanogels is different from that illustrated in Scheme 2. It is probably because of the formation of disulfide bonds between inter-nanogels instead of intra-nanogels.

DLS results showed that BImIL-based nanogels can respond to DTT obviously. Therefore, RhB was selected as the model drug to investigate the controlled encapsulation and release triggered by redox reaction. The drug loading efficiency (DLE) was calculated according to a working curve determined by UV-Vis spectrum. Due to the hyper cross-linked structure of BImIL-based nanogels, only very few RhB (less than 10%) could be loaded when it was incubated with the particles directly, which are probably absorbed on the surface of nanogels. To improve the drug loading efficiency, BVIm-based nanogels were firstly treated by DTT before the drug loading. Then, the drug RhB was added, and the solution was incubated for 24 h under nitrogen atmosphere. The mixture solutions were further treated by BPO to trap the cargos through the formation of disulfide bonds, and the free RhB were removed by dialysis from deionized water. The results are summarized in Table 2, it can be seen that both DLE and DLC increase obviously, which demonstrates that cleavage and formation of disulfide bond is a feasible technique to encapsulate the cargos for BVIm-based nanogels. Moreover, both DLC and DLE decrease with the increase of monomer [C_nVIm]Br (n=4, 6) in the feed ratio. It likely results from the lower containing of disulfide bond in the nanogels with the increase of [C_nVIm]Br

Table 2 DLE and DLC of RhB loaded in BImIL-based nanogels.

Entry	[C_nVIm]Br	Feed ratio[a]	D_h (μm)[b]	Zeta (mV)[c]	DLC wt%	DLE wt%
NG1	[C_4VIm]Br	5:1	0.67	7.1	10.3	60.5
NG2	[C_4VIm]Br	10:1	1.26	8.2	9.5	58.4
NG3	[C_4VIm]Br	15:1	1.74	14.1	8.6	58.1
NG4	[C_4VIm]Br	20:1	1.81	13.8	7.5	57.3
NG5	[C_6VIm]Br	5:1	0.75	7.8	10.9	64.3
NG6	[C_6VIm]Br	10:1	1.16	10.2	10.1	62.1
NG7	[C_6VIm]Br	15:1	1.38	12.2	9.6	59.3
NG8	[C_6VIm]Br	20:1	1.50	12.6	8.4	58.9
NG9	[C_6VIm]Br	30:1	1.72	11.9	8.0	58.7

[a] molar ratio of [C_nVIm]Br to DSDMA. [b] D_h of RhB lodaded nanogel; [c] ζ-potential of RhB loaded nanogel.

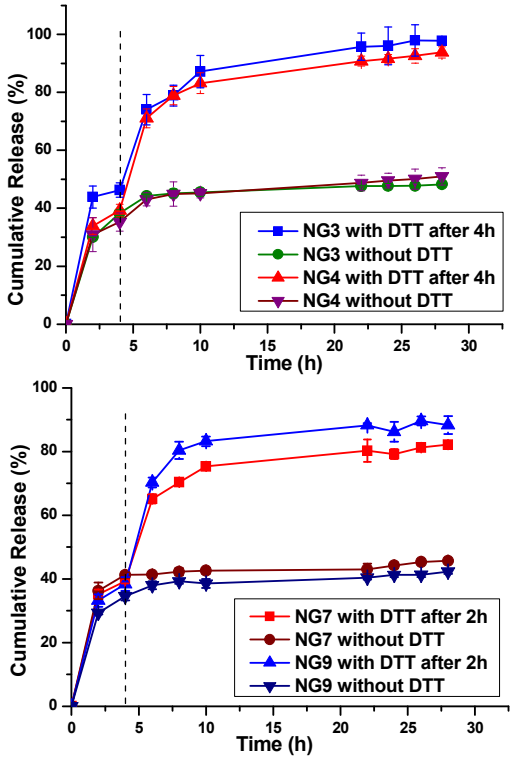

Figure 5 RhB release from BImIL-based nanogels in 7.4 buffer solution with and without DTT.

in the feed. As a result, the nanogels will be still hyper cross-linked after the disulfide cleavage, which is unfavorable to RhB encapsulation. On the contrary, more disulfide bonds will be favorable to the swelling of nanogels after DTT treatment, and RhB will pervade easily into the nanogels. The sizes of RhB-loaded nanogels were also checked by DLS. As indicated in Table 2, the diameters of RhB- loaded nanogels become much bigger than the nanogels without drugs, which should be because of the formation of disulfide bonds between nanogels in the process of BPO treatment. Moreover, there is no significant change on the ζ-potential after RhB was loaded.

Figure 5 shows the accumulative release of RhB from nanogels composed of different ratios of BImIL to DSDMA in PBS solution (pH=7.4). The results illustrate that only less than 50% RhB can be released from the nanogels in the absence of DTT after 28 h incubation. The released RhB are possibly those absorbed on the surface of nanogels. However, over 80% RhB could be released in the same duration in the presence of DTT. The result suggests that both RhB absorbed on the surface and embedded in the interior of nanogels can be released in the presence of DTT. A redox-triggered loading and release matrix has been successfully achieved by cross-linking copolymerization of BImIL-based monomers and DSDMA in selective solvent.

Conclusions

In summary, novel redox responsive nanogels have been developed readily by one-step cross-linking copolymerization of [C_nVIm]Br (n= 4 and 6) and DSDMA in selective solvent. The results illustrated that these novel BImIL-based nanogels can response to the redox stimuli, which would result in the size change of nanogels. By use of this virtue of BImIL-based nanogels, model cargo RhB could be uploaded under the reduction conditions. And the drug-loaded particles were further oxidized to form the disulfide bonds again, which could prevent cargos from leakage. Only less than 50% RhB could be released in the absence of DTT, while over 80% RhB could be released with the addition of DTT. This high cargos release is definitely attributed to the cleavage of disulfide bonds in reducing environments. Therefore, the novel redox-responsive nanogels could selectively increase intracellular drug release and potentially used as controlled carrier in biological medicine.

Acknowledgements

The authors are grateful for the financial support given by the National Natural Science Foundation of China (Project No. 21164008, 21474080) and Natural Science Foundation of Gansu Province (Project No. 1208RJZA167). Program for Changjiang Scholars and Innovative Research Team in University of Ministry of Education of China (Project No. IRT1177), Scientific and Technical Innovation Project of Northwest Normal University (nwnu-kjcxgc-03-63).

Notes and references

1 M. A. C. Stuart, W. T. S. Huck, J. Genzer, M. Müller, C. Ober, M. Stamm, G. B. Sukhorukov, I. Szleifer, V. V. Tsukruk, M. Urban, F. Winnik, S. Zauscher, I. Luzinov, S. Minko, *Nat. Mater.*, 2010, **9**, 101.
2 H. Lee, J. Pietrasik, S. S. Sheiko, K. Matyjaszewski, *Prog. Polym. Sci.*, 2010, **35**, 24.
3 N. Rapoport, *Prog. Polym. Sci.*, 2007, **32**, 962.
4 S. K. Ahn, R. M. Kasi, S. C. Kim, N. Sharma, Y. X. Zhou, *Soft Matter*, 2008, **4**, 1151.
5 A. Lendlein, and V. P. Shastri, *Adv. Mater.*, 2010, **22**, 3344.
6 D. Roy, J. N. Cambre, and B. S. Sumerlin, *Prog. Polym. Sci.*, 2010, **35**, 278–301.
7 X. Z. Yan, F. Wang, B. Zheng, and F. H. Huang, *Chem. Soc. Rev.*, 2012, **41**, 6042.
8 H. Y. Wen, H. Q. Dong, W. Xie, Y. Y. Li, K. Wang, G. M. Pauletti, D. L. Shi, *Chem. Commun.* 2011, **47**, 3550.
9 J. Dai, S. Lin, D. Cheng, S. Zou, X. Shuai, *Angew. Chem. Int. Ed.*, 2011, **50**, 9404.
10 F. Meng, W. E. Hennink, Z. Zhong, *Biomaterials*, 2009, **30**, 2180.
11 Y. Gao, J. Lu, J. Wu, J. Hu, Y. Ju, *RSC Adv.*, 2014, **4**, 63539.
12 M. Huo, J. Yuan, L. Tao, Y. We, *Polym. Chem.*, 2014, **5**, 1519.
13 T. M. Allen, P. R. Cullis, *Science*, 2004, **303**, 1818.
14 L. Gao, Q. Luo, Y. Wang, H. Du, X. Li, Z. Shen, W. Zhu, *RSC Adv.*, 2014, **4**, 4177.
15 H. Koo, G. W. Jin, H. Kang, Y. Lee, H. Y. Nam, H. S. Jang, J. S. Park, *Int. J. Pharm.*, 2009, **374**, 58.
16 S. Cerritelli, D. Velluto, J. A. Hubbell, *Biomacromolecules.* 2007, **8**, 1966.
17 H. Sun, B. Guo, X. Li, Z. Zhong, *Biomacromolecules.* 2010, **11**, 848.
18 F. Q. Schafer, G. R. Buettner, *Free Radic. Biol. Med.*, 2001, **30**, 1191.

19 Y. Lee , H. Mo, H. Koo, J. Y. Park, M. Y. Cho, *Bioconjug. Chem.*, 2007, **18**, 13.
20 H. Sun, B. Guo, R. Cheng, F. Meng, H. Liu, Z. Zhong, *Biomaterials.*, 2009, **30**, 6358.
21 R. Cheng, F. Feng, F. Meng, C. Deng, J. Feijen, Z. Zhong, *J. Control. Release*, 2011, **152**, 2.
22 H. Sun, B. Guo, R. Cheng, F. Meng, H. Liu, Z. Zhong, *Biomaterials.*, 2009, **30**, 6358.
23 L. Y. Tang, Y. C. Wang, Y. Li, J. Z. Du, J. Wang, *Bioconjug., Chem.* 2009, **20**, 1095.
24 Y. C. Wang, F. Wang, T. M. Sun, J. Wang, *Bioconjug. Chem.*, 2011, **22**, 1939.
25 J. Liu, Y. Pang, W. Huang, X. Huang, L. Meng, D. Yan, *Biomacromolecules.* 2011, **12**, 1567.
26 N. Ashwinkumar, S. Maya, R. Jayakumar, *RSC Adv.*, 2014, **4**, 49547.
27 J. K. Oh, D. I. Lee, J. M. Park, *Prog. Polym. Sci.*, 2009, **34**, 1261.
28 T. B. Ren, Y. Feng, Z. H. Zhang, L. Li, Y. Y. Li, *Soft Matter.*, 2011, **7**, 2329.
29 T. Thambi, H. Y. Yoon, K. Kim, I. C. Kwon, C. K. Yoo, J. H. Park, *Bioconjug. Chem.*, 2011, **22**, 1924.
30 V. I. Parvulescu, C. Hardacre, *Chem. Rev.* 2007, **107**, 2615.
31 T**.** Welton**,** *Chem. Rev.*, 1999, **99**, 2071.
32 J. Yuan, D. Mecerreyes, M. Antonietti, *Prog. Polym. Sci.*, 2013, **38**, 1009.
33 F. Endres, D. R. MacFarlane, H. Ohno, B. Scrosati, *Nat. Mater.*, 2009, **8**, 621.
34 L. Gao, Y. Yao, S. Dong, J, Yuan, *RSC Adv.*, 2014, **4**, 35489.
35 R. D. Rogers, K. R. Seddon, *Science*, 2003, **302**, 792.
36 Y. Kohno, Y. Deguchi, H. Ohno, *Chem. Commun.* 2012, **48**, 11883.
37 Y. Kohno, S. Saita, Y. Men, J. Yuan, H. Ohno, *Polym. Chem.* 2015, **6**, 2163.
38 Y. Men, X. H. Li, M. Antonietti, J. Yuan, *Polym. Chem.*, 2012, **3**, 871.
39 Y. Xiong, H. Wang, R. Wang, Y. Yan, B. Zheng, Y. Wang, *Chem. Commun.*, 2010, **46**, 3399.
40 Y. Xiong, Y. Wang, H. Wang, R. Wang, *Polym. Chem.*, 2011, **2,** 2306.
41 Y. Xiong, J. Liu, Y. Wang, H. Wang, R. Wang, *Angew. Chem. Int. Ed.*, 2012, **51**, 9114.
42 Y. Zuo, N. Guo, Z. J. Jiao, P. F. Song, X. J. Liu, R. M. Wang, Y. B. Xiong, *J. Polym. Sci. Part A: Polym. Chem.*, 2015, DOI: 10.1002/pola.27789.
43 X. F. Yuan, A. Harada, Y. Yamasaki, K. Kataoka, *Langmuir,* 2005, **21**, 2668.
44 W. A. Zhang, X. C. Zhou, H. Li, Y. Fang, G. Z. Zhang, *Macromolecules*, 2005, **38**, 909.
45 S. R. Deshiikan, K. D. Papadopoulos, *Colloid Polym. Sci.*, 1998, **276**, 117.
46 Y. T. Li, S. P. Armes, *Macrolecules*, 2005, **38**, 8155.
47 G. Valacchi, G. Rimbach, C. Saliou, S.U. Weber, L. Packer, *Toxicology*, 2001, **165**, 225.
48 J.F. Zhao, M. Lahiri-Chatterjee, Y. Sharma, R. Agarwal, *Carcinogenesis*, 2000, **21**, 811.

TOC Graphic

A redox-responsive nanogel matrix was fabricated by one-step synthesis for the controlled loading and release of cargos.